Proceedings of Ninth World Conference on Earthquake Engineering
August 2-9, 1988, Tokyo-Kyoto, JAPAN (Vol.IV)

6-6-17

EXPERIMENTAL STUDY ON THE DYNAMIC RESISTANCE MECHANICS IN R/C MULTISTORY PLANE FRAME STRUCTURE AGAINST STRONG BASE MOTION INPUTS

Hideo ARAKI[1] and Takayuki SHIMAZU[1]

[1]Department of Structural Engineering, Hiroshima University,
Saijo-cho, Higashihiroshima-shi, Japan

SUMMARY

Shaking table tests were conducted with an aim to verify the validity of the newly proposed limit state design method. Scaled down plane frame models were subjected to sinusoidal or earthquake base motions. It was found that the proposed limit state design method is very effective in controlling the displacement distributions over the height of frames in addition to the merit of the easiness of construction.

INTRODUCTION

Frame systems should be designed to be of beam collapse mechanism to avoid the occurrence of "soft story" (Ref.1,2,3). But it is difficult to design a frame to be of weak beam-strong column type, due to the insufficient understanding, at present stage on cooperative effects (Ref.4) of slab reinforcement as well as the simultaneous development of plastic hinges in all the beams that frame into the column when subjected to skew earthquake attack (Ref.3). The limit state design method (LDM) proposed in this paper is considered to replace the currently used elastic analysis method (EAM). The frame designed according to LDM is in such way that the flexural strength at plastic hinge in beams are arranged uniformly over the height of the building with total value of strength being the same as in the frame designed by EAM for the easiness of construction as well as that of control of safety factor over the height of building.

TEST PROGRAM

Proposed Design Method The strength at plastic hinge in all beams in the newly proposed limit state design method is designed based on the following equation.

$$Mby = \{ \sum_{i=1}^{n} (Q_{UD} + hi) \} / (n+k) \qquad (1)$$

Mby : design beam strength
Q_{UD} : design story shear force (Ds·Qui)
h : height of story
n,k : number of beams and ratio of beam strength to column strength

where, Ds is the structural coefficient for ultimate strength design representing energy absorbtive capacity of the structure related with ductility and damping for each story. Eq.(1) represents that of the equilibrium of moment at base.

Table 1 Cross Section for Members

Member of Test Structure		Story	b×D (mm)	I (cm⁴)	Tensile Reinforcement
Beams	FL8 type	1-8	50×25	6.51	2-3.2φ pt=1.07%
	FC8 type	7-8	40×20	2.67	3-2.3φ pt=1.56%
		5-6	40×25	5.21	2-3.2φ pt=1.60%
		3-4	60×25	7.81	3-3.2φ pt=1.60%
		1-2	60×30	13.5	3-3.2φ pt=1.34%
Columns	Interior	1-8	60×30	13.5	2-3.2φ pt=0.89%
	Exterior	1-8	60×40	32.0	2-3.2φ pt=0.67%

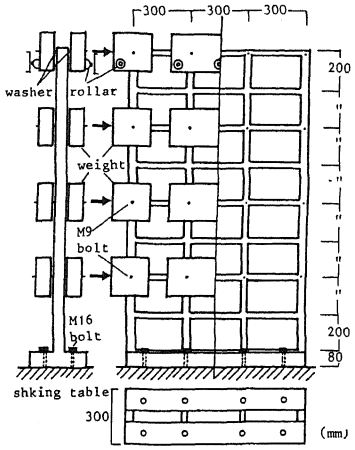

Fig.1 Test Apparatus and Details of Test Structure

Table 2 Strength of Members

Test Structure	Story	Beams My‡ (ton·cm)	Interior cMu‡‡ / My	Exterior cMu‡‡ / My
FL8 type	7-8	1.27	1.43	1.91
	5-6		1.50	2.00
	3-4		1.56	2.09
	1-2		1.63	2.18
FC8 type	7-8	0.60	3.03	4.04
	5-6	1.10	1.97	2.51
	3-4	1.52	1.31	1.75
	1-2	1.91	1.08	1.45

‡ My=0.9·at·σy·d for Beams
‡‡ cMu=0.8·at·σy·D+ 0.5N·D{1-N/(b·D·Fc)} for Columns

Table 3 Mechanical Properties for Concrete

Test Structure	Base Motion	Compressive Strength Fc(kg/cm²)	Young's Modulus * E(kg/cm²)
FL8-S FC8-S	Sinusoidal Base Motion	380 402	2.70×10^5 2.24×10^5
FL8-E FC8-E	Earthquake Base Motion	443 374	2.84×10^5 2.92×10^5

* at 1/4 Fc for concrete

Test Structures The one-sixteenth scaled 8-story 3 span reinforced concrete plane frame structures were tested. Two kinds of test structures, one designed with LDM (FL8 type) and the other designed with EAM (FC8 type), were prepared. In design procedure, first, test structures (FC8 type) were designed by currently used design method. Secondly, flexural strength of beam (Mby) for FL8 type were designed with Eq.(1) using story shear force Q_{UD} used in currently design method. The flexural strength (Mby) of beams are arranged uniformly over the height of the building with total value of strength being the same as in the frame FC8 type. Cross sections and strength for members are tabulated in Table 1 and Table 2 respectively. A typical test structure (FL8 type) with dimension is illustrated in Fig.1. The test structures were cast horizontally into metal form by the same batch of concrete. River sand of 3.2 mm maximum size was used in concrete. The mechanical properties of concrete is listed in Table 3. The reinforcement used in the fabrication of test structures were of the diameter 1.0, 2.3 and 3.2 mm and their yield strength were 4070, 5750 and 4480 (kg/cm^2) respectively.

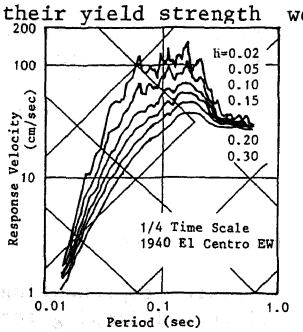

Fig.2 Response Spectra

Table 4 Maximum Acceleration of Base Motion Input at Each Run Level

(a) Sine Wave

Test Structure	Freq.	5 c/s			4 c/s			3 c/s			2 c/s
	Amp.	10	30	50	10	30	50	10	30	50	100
FL8-S		50	205	324	86	187	299	30	75	200	112
FC8-S		50	260	413	66	187	279	30	110	191	125

(b) Earthquake Wave

Test Structure	Run 1	Run 2	Run 3	Run 4	Run 5
FL8-E	564.	960.	1082.	1520.	1473.
FC8-E	577.	952.	1215.	1504.	1547.

unit ; cm/sec²

Test Procedure Dynamic tests were conducted using the shaking table with both sinusoidal and earthquake base motion inputs. Two test structures were subjected to a series of sinusoidal base motions to make resonance phenomena at each input level with aim to obtain the fundamental dynamic behavior of multistory plane frame from elastic range to post yielding. The other two test structures were subjected to a series of one-fourth scaled recorded earthquake (1940 El Centro EW) taking into account the scale effects for the test structures. Response spectra of this recorded earthquake base motion at Run 4 are illustrated in Fig.2. The amplitude of earthquake waves were increased in four steps. Maximum accelerations of both base motion inputs at each Run level are listed in Table 4.

EXPERIMENTAL RESULTS AND DISCUSSIONS (SINUSOIDAL BASE MOTIONS)

Crack Patterns Flexural cracks were observed at beam ends of the lower part of FL8-S, at early stages but overall crack patterns observed do not show significant variation in both types of test structures of FC8-S and FL8-S.

Acceleration Distributions The acceleration distributions at maximum base shears at each input level are shown in Fig.3(a). Base shear was obtained as follows.

$$\text{Base Shear} = \sum_{i=1}^{n} mi\ (\ddot{x}i + \ddot{x}o) \qquad (2)$$

mi : mass of the ith story
$\ddot{x}i+\ddot{x}o$: absolute acceleration of the ith story
n : total number of story

Although input levels for both test structures type were the same, magnification factors for acceleration of FL8-S were small at last stage because more energy absorption at end of all beams were expected in this type of structures.

Displacement Features The lateral displacement distributions at maximum top level displacement at each input level are shown in Fig.3(b). The lateral distribution were inverted-triangular and did not change throughout the test. At first stage, displacement of lower part for FL8-S within elastic range was larger than that for FC8-S because reinforcement of those parts was designed relatively poor. But, at last stage, displacement of top level for FL8-S was smaller than that of FC8-S because of large energy dissipation. In any case, there was no outstanding difference for responses between both type of test structures, because the first mode was always excited.

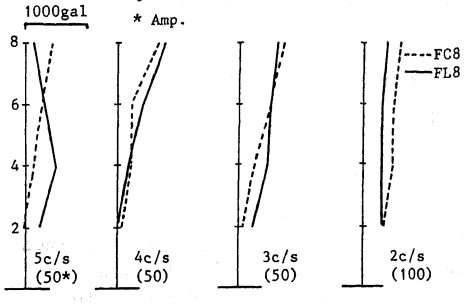

Fig.3(a) Lateral Acceleration Distributions for Sine Wave

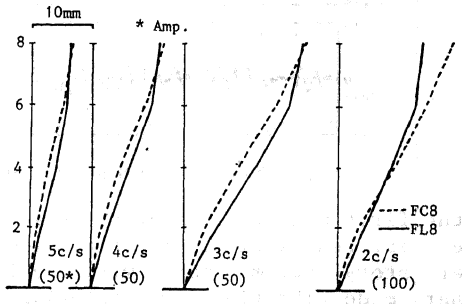

Fig.3(b) Lateral Displacement Distributions for Sine Wave

EXPERIMENTAL RESULTS AND DISCUSSIONS (EARTHQUAKE BASE MOTIONS)

Crack Patterns Remarkable cracks were observed at beam ends of the upper stories for FC8-E. The splitting of cover concrete as well as flexural cracks in

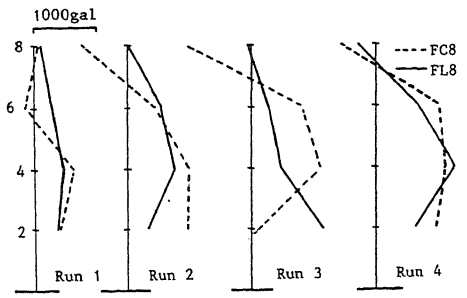

Fig.4(a) Lateral Acceleration Distributions for Recorded Earthquake Wave

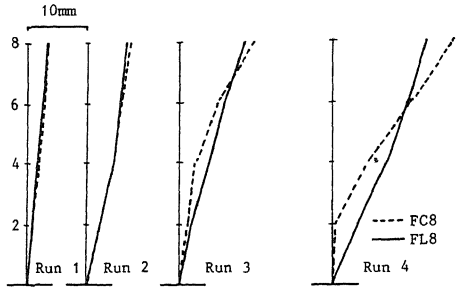

Fig.4(b) Lateral Displacement Distributions for Recorded Earthquake Wave

columns of these upper stories of the same structure was also observed. It may be due to the whipping phenomena observed during the test. Crack patterns of FL8-E was basically the same as those of FL8-S subjected to sinusoidal base motions.

Acceleration Distributions The acceleration distributions at each input level are shown in Fig.4(a). It was observed that the second mode was excited in those distributions at every input levels. This phenomenon was observed more clearly in FC8-E.

Displacement Features The lateral displacement distributions at each input level are shown in Fig.4(b). The remarkable difference between the both types of test structures were observed. The displacement distributions for FL8-E were vibrated

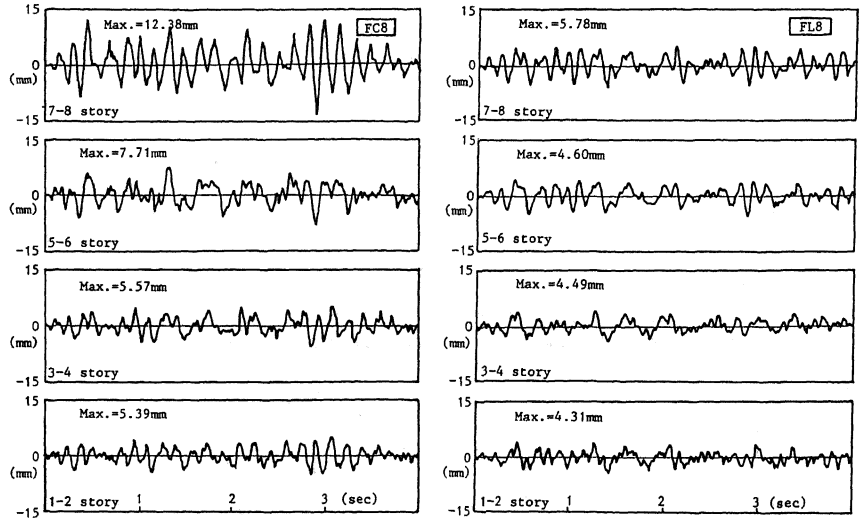

Fig.5 Observed Time Histories of Story Drifts for Recorded Earthquake Wave

in the first mode throughout the test. Although the distributions for FC8-E type were vibrated nearly in the first mode at initial stage, lateral displacement of upper story become large with the increase of input amplitude because of the higher mode vibration.Time histories of story drift at Run 4 are shown in Fig.5. Maximum story drift of the 7-8th story was two times as large as that of the other stories for FC8-E.

ANALYTICAL RESULTS AND DISCUSSIONS

Outline of Analytical Method The dynamic nonlinear frame analysis method (Ref.5)

was developed to predict the test results. A test structure was replaced by frame model with imaginary concentrated springs and rigid zone at the ends of the members as shown in Fig.6. Origin oriented model with tri-linear envelope curve was assumed as a hysteresis rule for each member of the test structure. Assumed model is shown in Fig.7. A step-by-step numerical integration procedure is used to solve the equations of motion for dynamic analysis of test structure. The equation of motion in terms of the relative displacements of the mass points to the base can be written in an incremental form as follows:

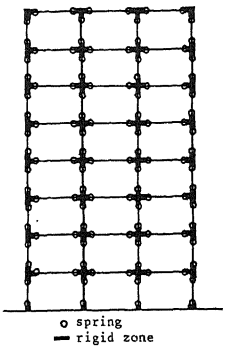

Fig.6 Mechanical Model for Test Structures

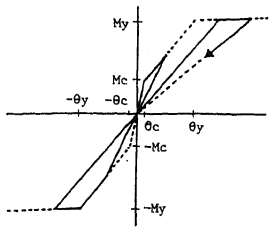

Fig.7 Assumed Restoring Force Characteristics

$$[M]\{\Delta\ddot{x}\} + [C]\{\Delta\dot{x}\} + [KH]\{\Delta x\} = -[M]\{\Delta\ddot{x}_o\} \qquad (3)$$

$[M]$: diagonal mass matrix
$[C]$: damping matrix
$[KH]$: structural stiffness matrix
$\{\Delta\ddot{x}\}, \{\Delta\dot{x}\}, \{\Delta x\}$: relative incremental acceleration, velocity and displacement vector, respectively
$\{\Delta\ddot{x}_o\}$: base acceleration vector

The implicit form of the Newmark Beta method with $\beta = 1/4$, a increment time T=0.005 sec., is chosen in this study. A damping matrix proportional to just the initial stiffness matrix is used. Overestimations due to usage of the initial stiffness matrix is acceptable because the damping effect should be expected to become larger when any inelastic action is occurring in the structure.

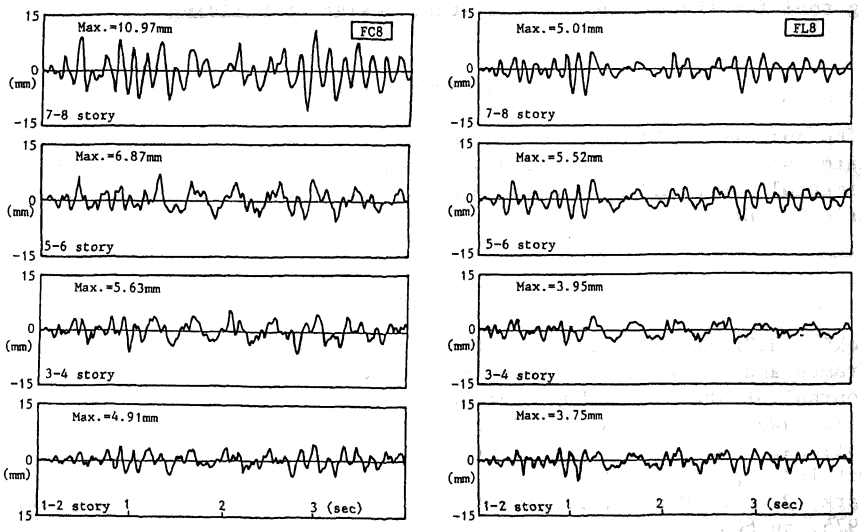

Fig.8 Calculated Time Histories of Story Drifts for Recorded Earthquake Wave at Run 4

Discussions for Calculated Results The calculated time histories of story drift for the test structures subjected to earthquake base motions are shown in Fig.8. Large story drift of the 7-8th story for FC8 type were observed in comparison with

those of the 1-6th story, which are about the same as experimental results. Ductility factors of beam ends and the bottom ends of columns are shown in Fig.9. Ductility factors of beams for FL8 type were uniformly distributed over the height of the test structure and average values were 2-3. Those of top beams for FC8 type becomes about 5. It should be noted that the ductility factor value of the 7th story column end for FC8 type was more than 1, although the strength ratios between column strength to beam strength were designed to be more than 3. It may be due to the higher mode vibration.

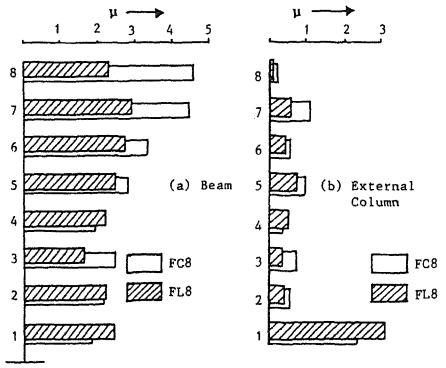

Fig.9 Calculated Ductility Factors

CONCLUSIONS

Shaking table test have been conducted to verify the validity of the newly proposed limit state design method (LDM) over the currently used elastic design method (EAM). The frame designed to LDM is in such way that the flexural strength at plastic hinge in beams are arranged uniformly over the height of the building. Based on the experimental and analytical results, the following conclusions can be made.

(1) There was no outstanding difference for responses between both types of test structures in the sinusoidal base motion test while remarkable difference was observed in the earthquake base motion test for the story drift between LDM and EAM types by the reason that the higher modes were excited in the upper part of EAM test structure with whipping phenomena.

(2) The dynamic nonlinear response was predicted with frame analysis. Good agreements have been found between observed and calculated time histories of story drift. It was concluded that the newly proposed design method is prospective as a strong tool for the earthquake resistant design of building.

ACKNOWLEDGEMENTS

The authors would like to express their thanks to C. Fujita and Y. Monji, the graduate students of the Hiroshima University for their cooperation. The experimental work had been performed by using the Earthquake Simulator of Chugoku Electric Co. Ltd.

REFERENCES

1. Seki, H."Relative Strength of Columns Necessary for Designing Weak-Girder RC Frames and Verification of the Simplified Analysis by Equivalent 1-DOF Model," Journal of Structural Engineering, Vol.31B, March,1985.
2. Kai, Kawatani, Aoyama and Otani," Moment of Columns of RC Frame which is Beam Collapse Mechanism Type during Earthquake," Annual Convention of AIJ, Oct,1982, pp.1511-1512.
3. Park, P. and Paulay, T.,"Reinforced Concrete Structures," John Willey & Sons, 1975, pp.603.
4. Suzuki, N., Otani, S. and Kobayashi, Y., "Three-Dimensional Beam-Column Subassemblages under Bidirectional Earthquake Loading," The Proc. of the Eighth World Conference on Earthquake Engineering, Vol.6, pp.453-460.
5. Emori, K. and Schinobrich, W.C.,"Analysis of Reinforced Concrete Frame Wall Structures for Strong Motion Earthquakes," Structural Research Series, No. 457, University of Illinois, Urbana, 1976.